

## Molecularly endowed hydrogel with in-silico-assisted screened peptide for high sensitive small molecules harvesting

Concetta Di Natale,<sup>a</sup> Giorgia Celetti <sup>a</sup>, Pasqualina Liana Scognamiglio <sup>a</sup>, Chiara Cosenza<sup>b</sup>,  
Edmondo Battista<sup>b</sup>, Filippo Causa <sup>a,b,c</sup>, Paolo A. Netti <sup>a,b,c</sup>

<sup>a</sup> Center for Advanced Biomaterials for Healthcare, Istituto Italiano di Tecnologia (IIT), Largo Barsanti e Matteucci 53, 80125 Naples, Italy

<sup>b</sup> Interdisciplinary Research Centre on Biomaterials (CRIB), University “Federico II”, Piazzale Tecchio 80, 80125 Naples, Italy

<sup>c</sup> Dipartimento di Ingegneria Chimica, dei Materiali e della Produzione Industriale (DICMAPI), University “Federico II”, Piazzale Tecchio 80, 80125 Naples, Italy

### Supporting Information

#### Table of contents

<b>1. Materials</b> .....	<b>3</b>
<b>2. Peptide synthesis</b> .....	<b>3</b>
<b>3. Computational Modeling.</b> .....	<b>4</b>
<b>3.1 The aflatoxin M1 structure</b> .....	<b>4</b>
<b>3.2 Computational Library design</b> .....	<b>5</b>
<b>3.3 Molecular dynamics simulation and Interaction Energy calculation</b> .....	<b>5</b>
<b>4. Surface Plasmonic Resonance (SPR).</b> .....	<b>7</b>
<b>5. Hydrogel Microparticles synthesis</b> .....	<b>10</b>
<b>5.1 Hydrogel Microparticles Recovery by washing steps and SEM (Scanning electron microscopy) characterization</b> .....	<b>11</b>
<b>6. Fluorescamine assay</b> .....	<b>12</b>
<b>7. Hydrogel Microparticles counts</b> .....	<b>14</b>
<b>8. Confocal Microscopy and AFM1-BSA detection both in PBS and in Milk</b> .....	<b>14</b>
<b>9. AFM<sub>1</sub>-BSA conjugated detection in Milk using different concentrations of Hydrogel Microparticles</b> .....	<b>18</b>
<b>10. AFM<sub>1</sub> detection directly in Milk</b> .....	<b>19</b>

<b>11. NDPR binding with different hydrophobic small molecules.....</b>	<b>19</b>
<b>12. LoD values calculations.....</b>	<b>20</b>

## 1. Materials

Poly(ethylene glycol) diacrylate (PEGDA, 700 MW), the non polar solvent light mineral oil and the non ionic detergent sorbitanmonooleate (Span 80) were purchased from Sigma Aldrich. Cross-linking reagent Darocur 1173 was purchased from Ciba. Reagents for peptide synthesis (Fmoc-protected amino acids, resins, activation, and deprotection reagents) were purchased from Iris Biotech GmbH (Marktredwitz, Deutschland) and InBios (Naples, Italy). 1-ethyl-3-(3-dimethylaminopropyl)carbodiimide hydrochloride(EDC),N-hydroxysuccinimide(NHS), aflatoxinM1 (AFM1) and the AFM1 conjugated bovine serum albumin protein (BSA–AFM1) were from Sigma-Aldrich. Solvents for peptide synthesis and HPLC analyses were purchased from Sigma-Aldrich; reversed phase columns for peptide analysis and the LC–MS system were supplied respectively from Agilent Technologies and Waters (Milan, Italy). All SPR reagents and chips were purchased from AlfaTest (Rome, Italy ). All chemicals were used as received.

## 2. Peptide synthesis

Peptide libraries and single peptides were prepared by the solid phase method on a 50  $\mu$ mol scale following the Fmoc strategy and using standard Fmoc-derivatized amino acids. Briefly, the synthesis were performed on a fully automated multichannel peptide synthesizer Biotage® Syro Wave™. Rink amide resin (substitution 0.71 mmol/g) was used as solid support. Activation of amino acids was achieved using a HBTU:HOBt:DIEA mixture (1:1:2), whereas Fmoc deprotection was carried out using a 40% (v/v) piperidine solution in DMF. All couplings were performed for 15 minutes and deprotection for 10 minutes. For peptides library, 8 different amino acids were chosen to build the library based on their chemical and physical properties. The selected amino acids for the library construction were Arg, Asn, Pro, Trp, Leu, Ala, Asp and Thr. Particularly, the libraries were simplified in terms of having a reduced number of compounds screened that were still capable of covering a wide chemical diversity. Indeed the small subset of amino acids has been rationally chosen to ensure a broad diversity of functional groups. In detail, for residues with very similar properties, only one was chosen (for example, Asn instead of Gln and Asp instead of Glu). Arg was chosen instead of Lys and His because, although they all have a net positive charge at neutral pH, Arg contains a unique guanidine group. Among other aromatic side chains, Trp was preferred to Phe and Tyr. Ala and Ile were chosen among the aliphatic side chains, while Pro for his imino acid properties. Thr, instead of Ser, was chosen for the ability to form hydrogen bonding. The resin (4.55g) was split into 64 different tubes and each reactor holds the combination of the eight amino acids, selected for the library construction. At the end of previously reported coupling procedures we obtained 64 different dipeptides that constituted the first peptide library. The dipeptide with the best binding properties (selected by SPR technique and interaction energy calculation) was chosen as starting point at the C-terminal for the preparation of a tetrapeptide library. Thus we split the dipeptide-functionalized resin into 64 different tubes and we add other two residues at the N-terminus, combining the same eight building blocks. The higher affinity tetrapeptides were functionalized with Rhodamine to monitor their entrapment in PEG microparticles (Figure S10 in the following pages). In particular, the Rhodamine labeling of the amine in Lysine

side chain was achieved by on-resin treatment with Rhodamine Isothiocyanate (TRITC), after removing methyltrityl (Mtt) protecting group using 1% TFA in DCM for 30 min. The peptide library scheme was reported in the Figure S1.

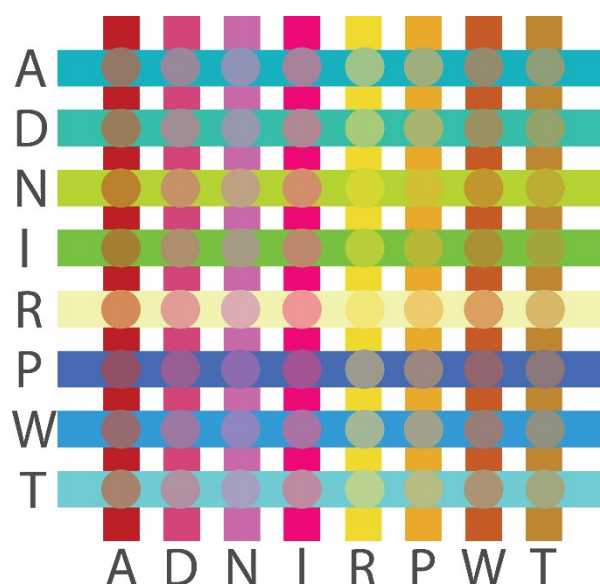


**Figure S1:** Schematic representation of the parallel peptide simplified library (one amino acid for each chemical-physical property): 8x8 amino-acids library matrix = 64 possible dipeptides. The same scheme was used for the construction of the tetrapeptide library for defining the third and fourth position.

### 3. Computational Modeling

The Computational Modeling selection was conducted using the Discovery Studio software package, version 4.5 (BIOVIA 5005 Wateridge Vista Drive, San Diego, CA 92121, USA).

#### 3.1. The AFM1 structure design

We drew the AFM1 molecule using the "Sketch and Edit molecules tools" inside the Discovery Studio (DS) software. The molecule was typed with the CHARMM force field available in the DS package and charges were added through the Momany-Rone method. The structure was minimized through 200 steps of energy minimization using the "Smart Minimizer algorithm" which performs Steepest Descent, followed by Conjugate Gradient minimization. In Figure S2 the AFM1 sketched structure was reported. Then we performed molecular dynamics simulation in NVT ensemble of the AFM1 in water box for 10 ns and we extracted the most populated structure in last 1 ns.

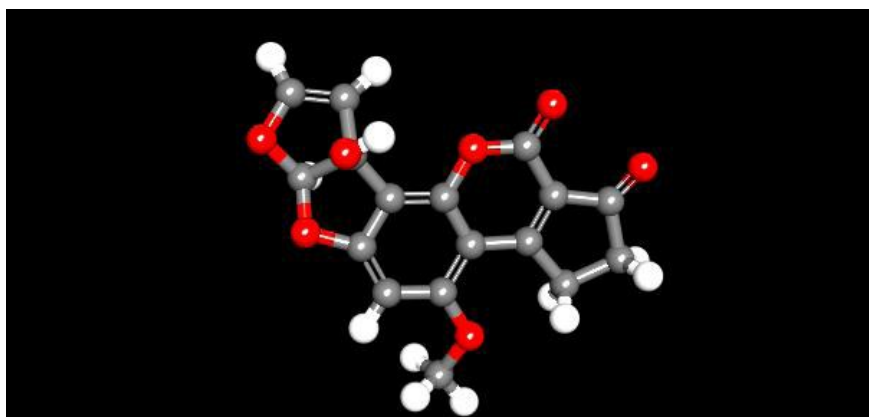


**Figure S2:** Aflatoxin M1 structure

### 3.2 Computational Library design

The computational library design was performed using a customized protocol to build peptides of a given length developed through the Pipeline Pilot software (version 9.5) following the flow chart reported in **Figure S3**. As in the experimental library construction, we used 8 amino acids as building blocks (Arg, Asn, Pro, Trp, Leu, Ala, Asp and Thr). The generated dipeptide library was validated using a computational approach composing by molecular dynamics and interaction energy calculation.

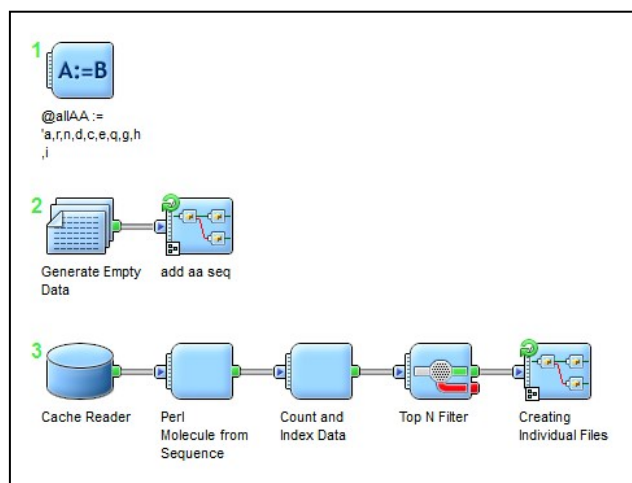


**Figure S3:** Flow chart of the protocol implemented in the Pipeline Pilot software used in this work to generate di- and tetra-peptide library.

### 3.3 Molecular dynamics simulation and Interaction Energy calculation

All the 64 peptides belonging to di- and tetra-meric libraries were typed with CHARMM force field and charged through the Momany-Rone method. We set 200 steps of energy minimization using the "Smart Minimizer algorithm", which performs Steepest Descent, followed by Conjugate Gradient minimization. Minimized peptide structures were solvated inside an orthorhombic water box ionized with a 0.145 M salt concentration.

We performed molecular dynamics simulation of the solvated peptides using the following protocol: an initial minimization stage using 1000 steps of Steepest Descent algorithm, a second minimization stage 2000 steps of Conjugate Gradient method, a 4 ps heating stage to increase the temperature from 50 K to 300 K, a 10 ps equilibration stage at 300 K and a production stage 1 ns molecular dynamics at 300 K in the NPT ensemble. The most populated conformations in last 1 ns from molecular dynamics were used as input receptor structures for interaction energy calculation against the AFM1. Afterwards we used CDocker<sup>1</sup>, a molecular dynamics simulated-annealing based algorithm, to generate 500 AFM1-peptide complexes poses with the highest score ranked according to the interaction energy<sup>2</sup>.

We reported the best docked poses for both the first and second screening in **Figure S4** and **S5**, respectively. The best AFM1 binding peptide was the NDPR sequence with an **Interaction Energy = -18.22**, among all the possible combinations we tested.

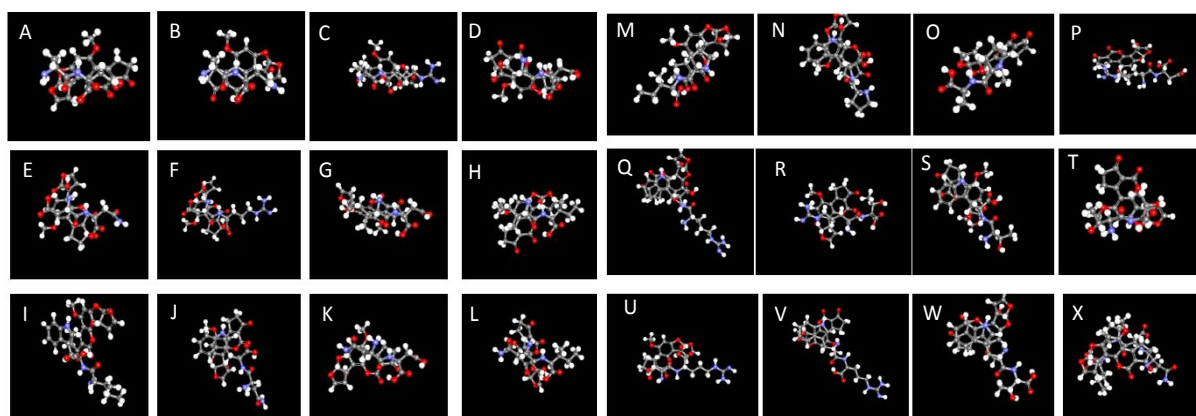


**Figure S4:** High affinity AFM1 binding di-peptide sequences selected at the end of computational approach: A)AD, B)AN, C)AR, D)DD, E)DN, F)DR, G)II, H)IN, I)IW, J)NI, K)NN, L)NW, M)PI, N)PW, O) PA, P) RW, Q) RT, R) RD, S)TW, T)TR, U)TT, V)WW, W)WR, X)WN.

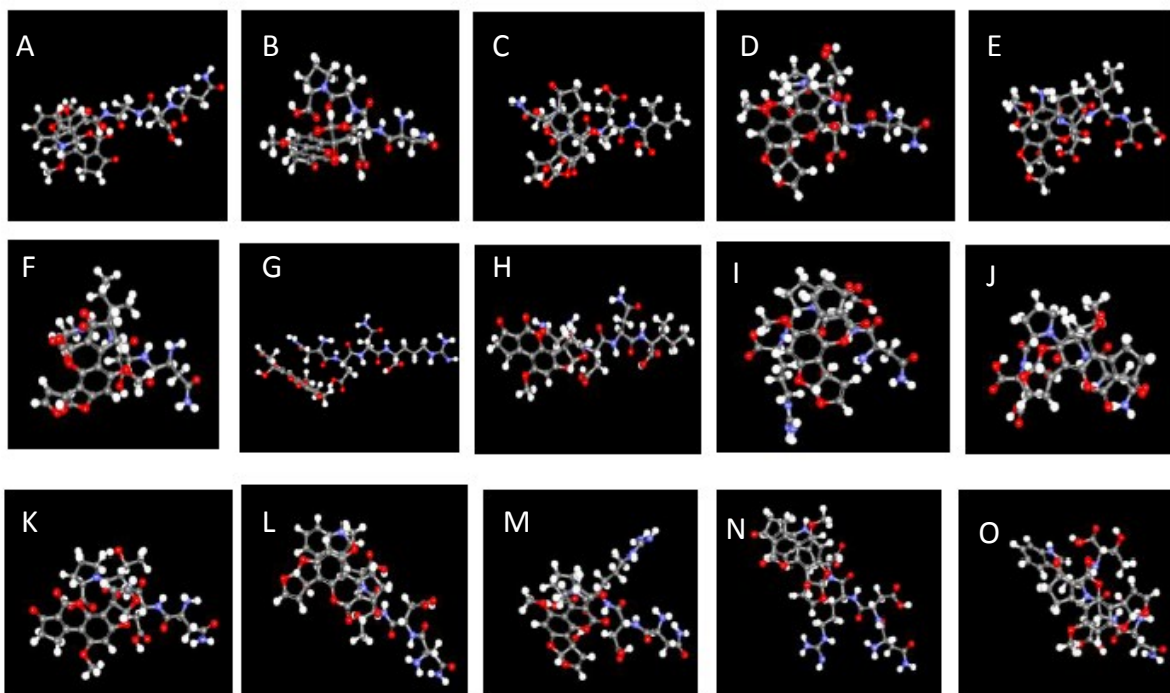


**Figure S5:** High-affinity AFM1 binding tetrapeptide sequences selected at the end of computational approach: A)NDAP,B)NDAW,C)NDDI,D)NDDP,E)NDID,F)NDIP,G)NDNR,H)NDNI,I)NDPR,J)NDPD,K)NDTP,L)NDTW,M)MDRP, N)NDRW,O)NDWN.

#### 4. Surface plasmonic resonance

In order to measure the affinity of the 64 di- and tetra-peptides (analyte) against the aflatoxin (ligand), we employed the SPR technique (SensiQ Pioneer from AlfaTest, Rome, Italy). AflatoxinM1-conjugated Bovine Serum Albumine (AFM1-BSA) was immobilized at a concentration of 50  $\mu\text{g}/\text{mL}$  in a 10 mM acetate buffer pH 3.7 (flow 10  $\mu\text{L}/\text{min}$ , injection time 20 min) on a COOH1 SensiQ sensor chip, using EDC/NHS chemistry (0.4 M EDC - 0.1 M NHS), flow 25  $\mu\text{L}/\text{min}$ , injection time 4 min), achieving a 7000 RU signal. Residual reactive groups were deactivated by treatment with ethanolamine hydrochloride 1 M, pH 8.5. To study the non-specific binding of peptides against BSA, the reference channel was activated with an EDC/NHS mixture and the BSA protein alone at a concentration of 50  $\mu\text{g}/\text{mL}$  is immobilized, reaching the same RU signal of the AFM1-BSA immobilization (7000). The binding assays were performed at 25  $\mu\text{L}/\text{min}$ , with a contact time of 4 min, and all peptides were diluted in the buffer stroke, HBS (10 mM Hepes, 150 mM NaCl, 3 mM EDTA, pH 7.4). The injection of analytes (100  $\mu\text{L}$ ) was performed at the indicated concentrations. The association phase ( $k_{\text{on}}$ ) was followed for 180 s, whereas the dissociation phase ( $k_{\text{off}}$ ) was followed for 300 s. The complete dissociation of the formed active complex was achieved by addition of a 10 mM NaOH solution, for 60 s before each new cycle start. We employed the software QDAT analysis package (SensiQ Pioneer, AlfaTest) to subtract the signal of the reference channel and evaluate the kinetic and thermodynamic parameters of the complex. In **Figure S6** the fitted sensorgram of the best AFM1 binding dipeptide (ND sequence) was reported.

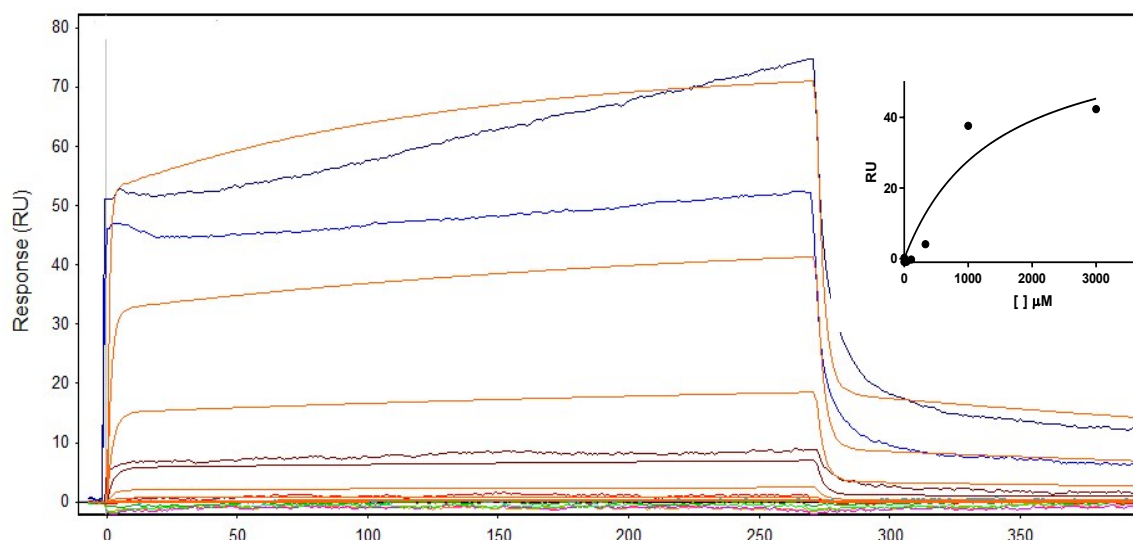


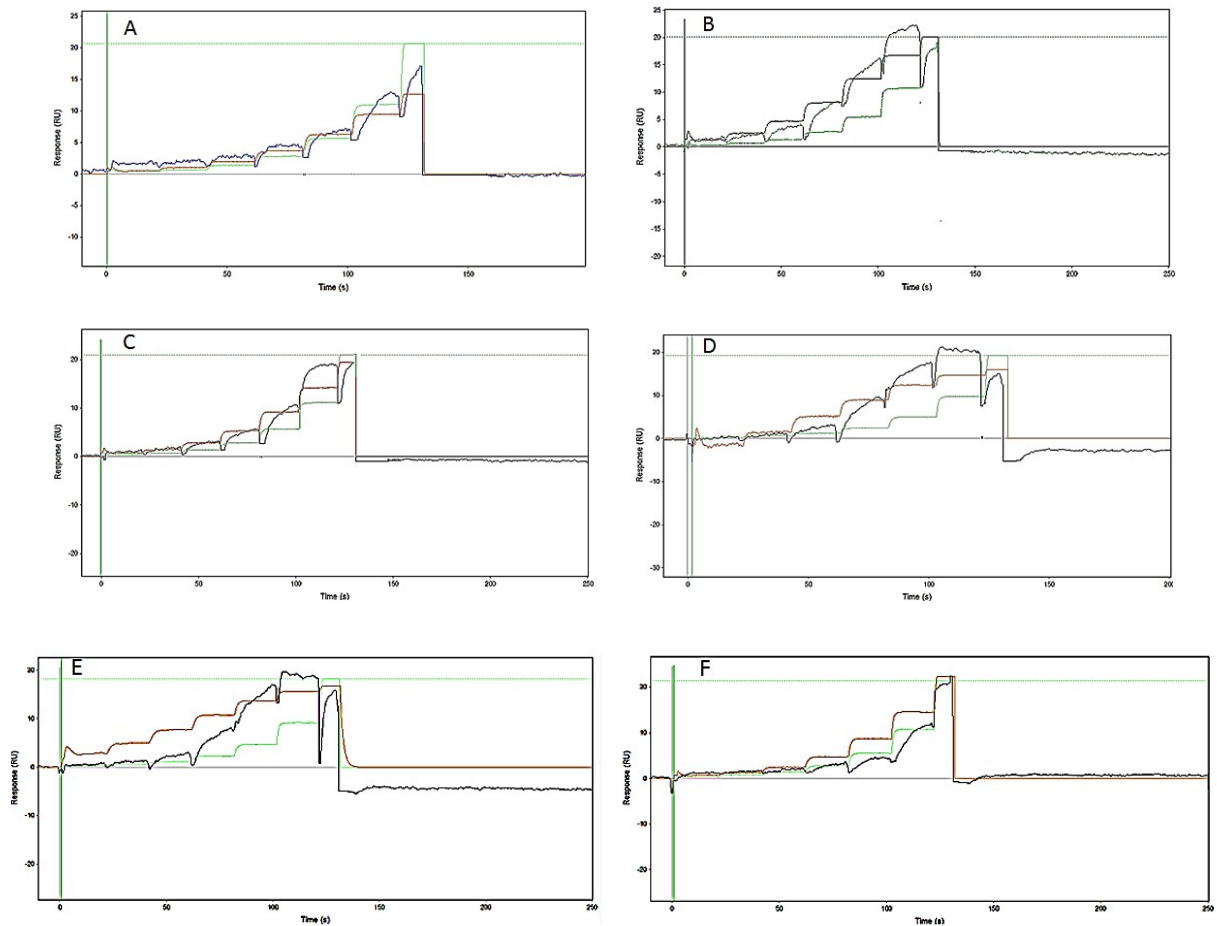
**Figure S6:** Conventional SPR experiment between ND peptide (analyte) and AFM1-BSA (ligand). Analyte concentration from 1.5  $\mu\text{M}$  to 3.0 mM. Employing a 1:1 interaction model, a  $K_D = 1.4 \pm 0.1\text{mM}$  was calculated. Inset: SPR signal at equilibrium as function of analyte concentrations; the relative fitting with a Langmuir binding isotherm model gives  $K_D = 1.4 \pm 0.95\text{mM}$ .

For tetrapeptide library, binding experiments were conducted by Fast step injection to eliminate the overhead associated with multiple loading, injecting and clean up cycles making substantial reductions in time and procedure complexity. In this case an analyte concentration of  $400\mu\text{M}$  was used with a flow rate of  $200\mu\text{L}/\text{min}$ , a contact time of 20 sec and a dissociate time of 120 sec. As to bulk standard cycles, a 20% of sucrose was used. Kinetic parameters for all tetrapeptides were estimated assuming a 1:1 binding model and using QDAT software for all analysis (SensiQ Technologies). In **Figure S7 a)** and **b)** the sensorgrams of the best six AFM1 binding tetrapeptides were shown and their affinity constants were reported in **Table S1**.

**Table S1:**  $K_D$  evaluation with kinetic and equilibrium parameters.

Best sequence	Kinetic parameters	Equilibrium parameters
	$K_D(\mu\text{M})$	$K_D(\mu\text{M})$
NDRN	$161 \pm 20$	$83.67 \pm 19.38$
NDRD	$49 \pm 100$	$123.8 \pm 50.68$
NDRP	$330 \pm 20$	$189.6 \pm 73.20$
NDNR	$98 \pm 30$	$100 \pm 10.10$
NDDR	$100 \pm 21$	$81.2 \pm 58.20$
NDPR	$710 \pm 20$	$611 \pm 27.0$

a)



b)

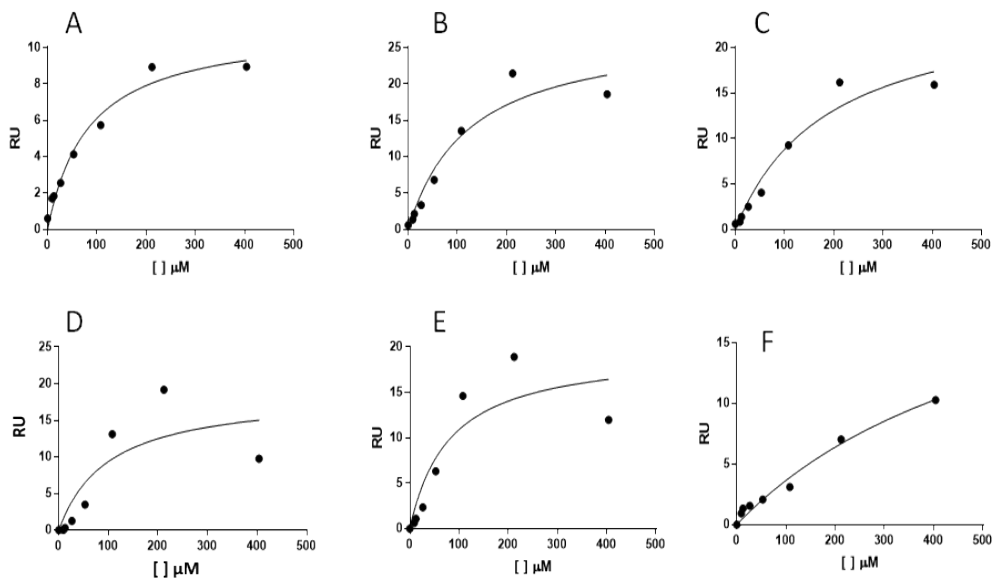


**Figure S7:**Fast step results of six tetrapeptides. (a) Fast step fitted sensorgrams using QDAT software and (b) Plot of SPR signal at equilibrium as function of analyte concentrations, fitted with the Langmuir binding isotherm. The sequences reported are: A) *NDRN*, B) *NDRD*, C) *NDRP*, D) *NDDR*, E) *NDNR*, F) *NDPR*. The  $K_D$  values are reported in **Table S1**.

## 5. Hydrogel Microparticles synthesis

Hydrogel Microparticles were synthesized using Light Mineral Oil (LMO) containing non-ionic surfactant Span 80 (3 wt%) as a continuous phase and a poly(ethylene glycol)diacrylate (PEGDA) solution (20 wt%) mixed with photoinitiator (0.1 wt%) and peptides (NDNRD-(O-allyl)), NDDRD-(O-allyl), NDPRD-(O-allyl)), (70 mg/L) solutions, as a disperse phase. So the peptides were opportunely functionalized with an allyl group (introduced as Fmoc-Asp(Oall)-OH). The Fmoc group was removed from the peptide at the end of the synthesis before its integration into hydrogels. Droplets were formed injecting the disperse phase through the central channel while the continuous phase through two opposite side channels. The device inlets and outlets were connected with polyethylene tubes, and the solutions were injected using high-precision syringe pumps (neMesys-low pressure) to ensure a reproducible, stable flow. This system was mounted on an inverted microscope (IX 71 Olympus) and droplet formation was visualized using a 4× objective and recorded with a CCD camera ImperxIGV-B0620M. The PEGDA-peptide droplets were crosslinked in-flow after exposition to UV light, to form monodisperse Hydrogel Microparticles. The UV light (9.8 mW) was filtered with DAPI microscopy filter ( $\lambda=360$  nm) and focused on the device. The diaphragm aperture of the microscope was used to limit exposure to the serpentine region of the chip. After photopolymerization, the Hydrogel Microparticles were collected in an eppendorf and washed three times with a solution of ethanol (35 v/v%) and acetone (10 v/v%) to remove the oil.

Rhodaminated peptides were used to control the homogenous distribution of peptide sequences into Hydrogel Microparticles. Fluorescence analysis was performed by Leica SP5 confocal microscope. Bright field and fluorescence images using a HCX IRAPO L 40×/0.95 water objective were acquired; 540 nm line of the Argon laser as excitation sources for Rhodamine-peptide was used and detection occurred at the 600-700 nm band. Images were acquired with a resolution of 1024 × 1024 pixels, zoom 1, 2.33A.U. and at maximum of pinhole (**Figure S8**). All our experiments were performed at room temperature.

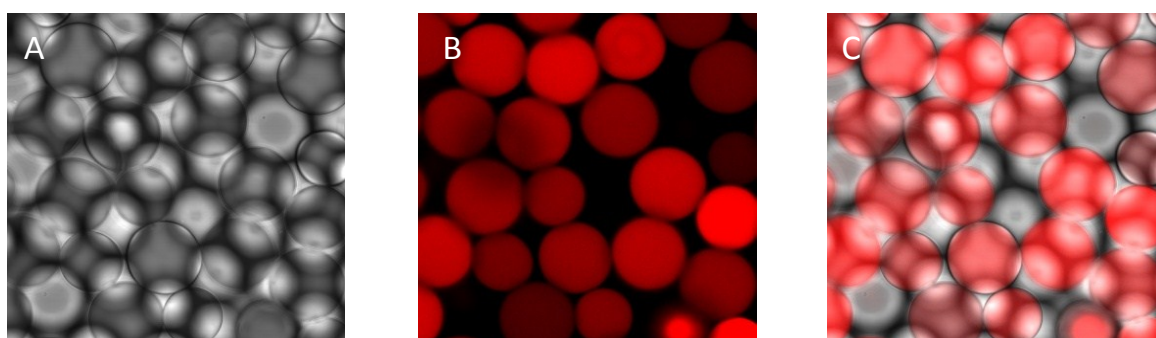


**Figure S8:** Confocal microscope images of Rhodamine-peptide Hydrogel Microparticles. A) Bright field and B) fluorescence images using a HCX IRAPO L 40×/0.95 water objective were acquired; 540 nm line of the Argon laser as excitation sources for Rhodamine-peptide was used and detection occurred at the 600-700nm band. C) Overlay of Bright field and fluorescent channels.

## 5. 1 Hydrogel Microparticles Recovery by washing steps and SEM (Scanning electron microscopy) characterization

Oil-dispersed Hydrogel Microparticles were recovered by an optimized washing protocol. Briefly, 1 mL of a mixed acetone/isopropanol/water solution (30:10:60) was added to the biphasic-system followed by centrifugation at 10000 rpm for 5 minutes, and repeated two times<sup>3</sup>. In this way, the supernatant containing oil was eliminated and Hydrogel Microparticles were re-suspended in PBS buffer pH 7.4 and stored at 4°C. In order to evaluate the effective oil removal, SEM characterization with EDS analysis (Energy Dispersive X-ray Spectroscopy) was performed. SEM analysis was performed with an Ultra Plus FESEM scanning electron microscope (Zeiss, Germany). 10  $\mu$ L of peptide Hydrogel Microparticles and control-Hydrogel Microparticles (without peptides incorporation) stock solution at 0.1mg/mL were mounted on microscope stubs, dried overnight and sputter coated with gold (approximately 7 nm thickness). In particular, washed Hydrogel Microparticles had a good sphericity and a rough surface (**Figure S9 a**) A-B-C-D). The roughness was due to use of dehydrating solvents. Water extraction appears to change the PEGDA Hydrogel Microparticles network. Unlike, not good sphericity and smooth surface was detected in not properly washed Hydrogel Microparticles. The smooth and dense Hydrogel Microparticles surface were due to residual surfactants and oil component (data confirmed also by UV spectra, not shown) (**Figure S9 b**) E-F-G-H), as it is possible to see in EDS experiments (**Figure S10 a**) and b)).

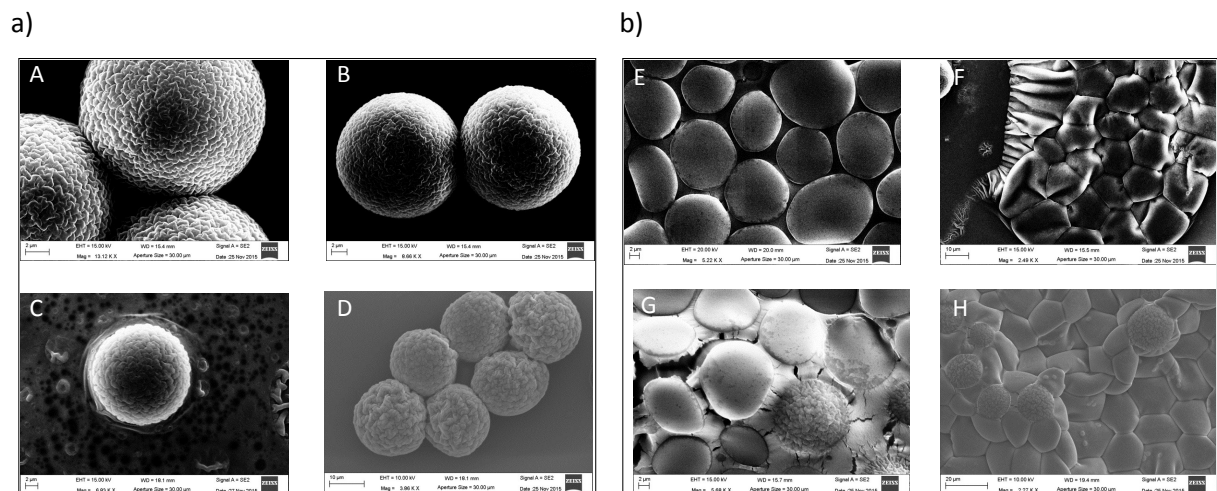


**Figure S9:** SEM images of peptide and control Hydrogel Microparticles. a) Washed Hydrogel Microparticles: the A) NDPR, B) NDNR, C) NDDR and D) control-Hydrogel Microparticles were represented. b) No washed Hydrogel Microparticles: the E) NDPR, F) NDNR, G) NDDR and H) control-Hydrogel Microparticles were represented.

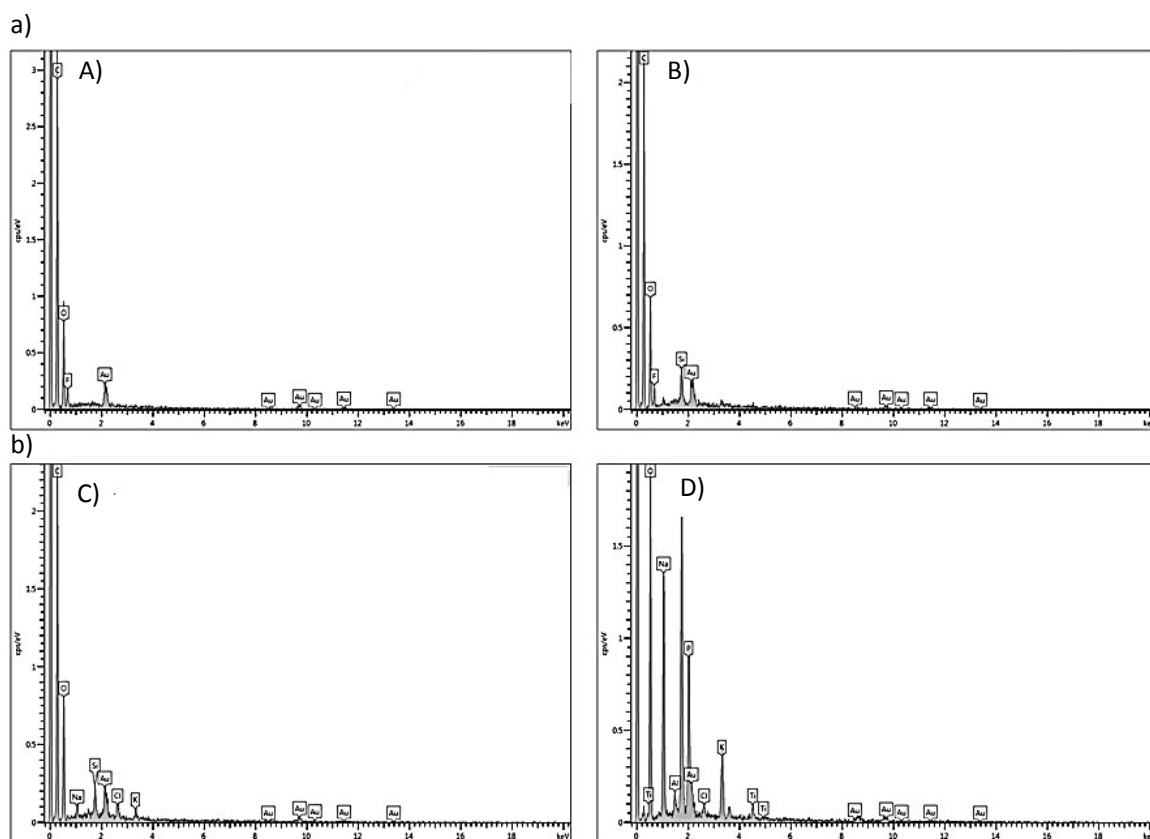


**Figure S10:** Example of EDS analysis of peptide-Hydrogel Microparticles and control-Hydrogel Microparticles . a) No washed Hydrogel Microparticles were represented: A) NDPR peptide- Hydrogel Microparticles and B) Control-Hydrogel Microparticles. b) The washed Hydrogel Microparticles were reported: C) NDPR peptide-Hydrogel Microparticles and D) Control-Hydrogel Microparticles .

## 6. Fluorescamine assay

Thanks to the presence of the free terminal  $\alpha$  amino group in all peptides synthesized, we evaluated the efficient and homogeneous peptide co-polymerization into Hydrogel Microparticles by a fluorescamine-based assay<sup>4</sup>. The non-fluorescent compound, fluorescamine, reacts rapidly with primary amines in proteins, such as the terminal amino group and the  $\epsilon$ -amino group of lysine, to form highly fluorescent moieties<sup>5</sup>. Fluorescamine was dissolved in HPLC grade acetone (3 mg/mL) to obtain a 1 mM solution. After 1 mL of 250  $\mu$ M solution of fluorescamine was added to Hydrogel Microparticles and mixed for 15 minutes. Sample was loaded in ibidichambers and fluorescence analysis was performed by multiphoton confocal laser scanning microscopy (Leica SP5) using a two photon laser at 700 nm. Objective: HCX IRAPO L 40.0x0.95 WATER section thickness 3  $\mu$ m, scan speed 400 Hz, excitation MP laser 700nm,  $\lambda_{em}$  range 500–540nm, image size 1024  $\times$  1024  $\mu$ m<sup>2</sup>, zoom 1, 2.33A.U. and 600 $\mu$ m pinhole. All experiments were conducted at room temperature. The fluorescamine assay was performed both for peptide Hydrogel Microparticles and control-Hydrogel Microparticles . All captured images were analyzed with a public domain image-processing program, IMAGEJ (v. 1.43i, NIH, Bethesda, MD, USA). The images were briefly thresholded by the Otsu algorithm and then processed with the ImageJ Analyze Particles function to computationally determine the number of single

fluorescent particles in the range of 20  $\mu\text{m}$ . The images were reported in **Figure S11** A-D and the quantification of Hydrogel Microparticles fluorescence was showed in **Figure S12**.

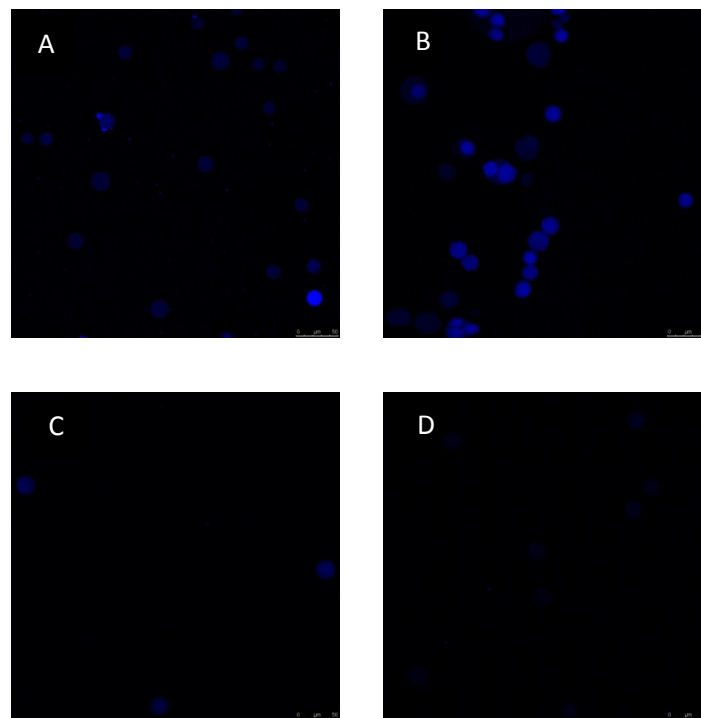


**Figure S11:** Fluorescamine assay. Multiphoton confocal laser scanning microscopy images, with excitation laser at 700nm. A-B-C) The fluorescence for Hydrogel Microparticles functionalized with NDDR, NDPR, NDNR peptides, respectively, was homogeneous. D) For control-Hydrogel Microparticles, the signal was very low, similar to the laser background.

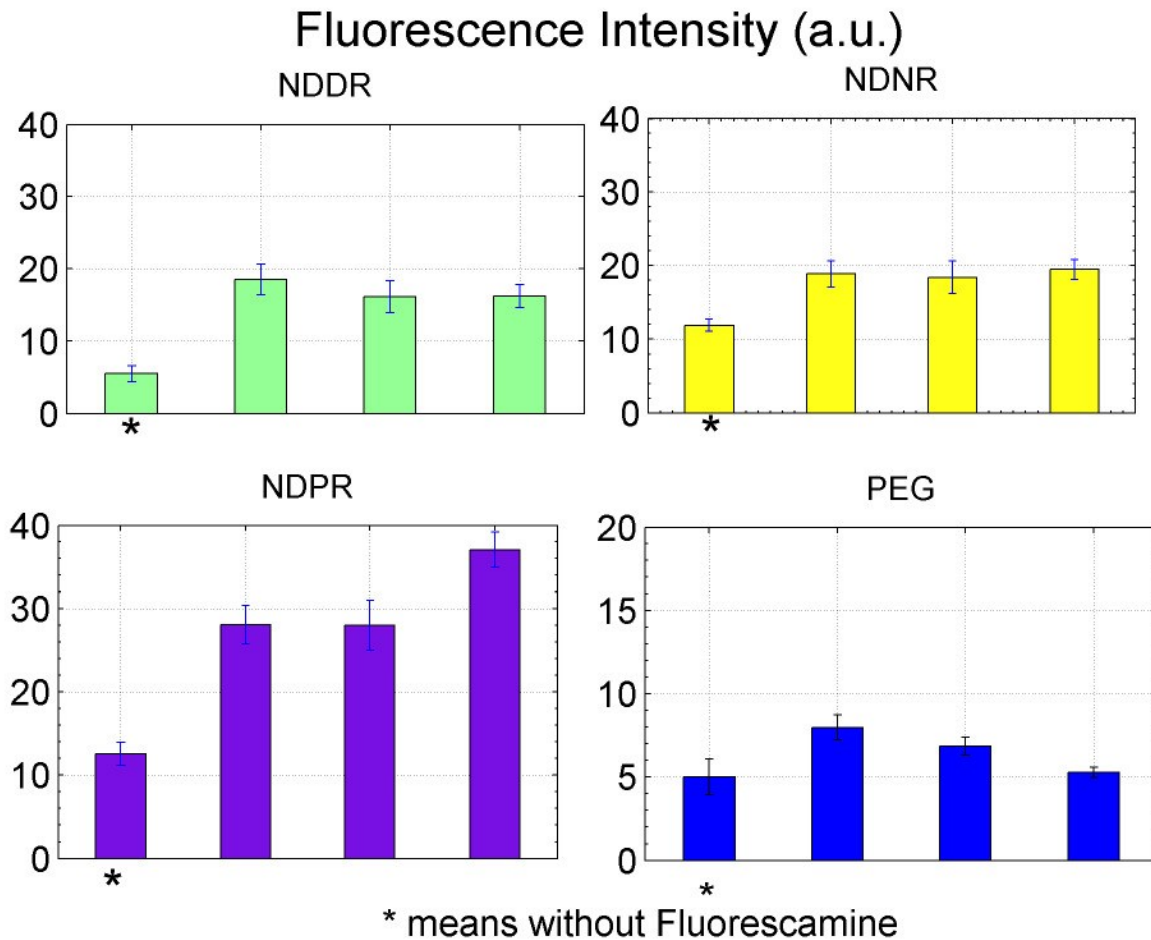


**Figure S12:** Fluorescence quantification by Image J tool. The amount of peptides into Hydrogel Microparticles was reproducible and homogeneous. The fluorescence signal of control-Hydrogel Microparticles was very low, similar to Hydrogel Microparticles without fluorescamine reaction.

### 7. Hydrogel Microparticles counts

Based on flow conditions, the yield of microgel production was around 300 microgel/minutes, thus the number of Hydrogel Microparticles synthesized was about  $2 \times 10^6$  particles/mL. This number was confirmed through the microgel calculation with a cell counting chamber (*FAST - READ 102-Biosigma s.r.l.*), after a dilution factor of 1:100. In particular, 7  $\mu\text{L}$  of Hydrogel Microparticles were loaded in each counting chamber and considering that the grid contains 10 squares and each square has a dimension of 1 x 1 mm, a depth of 0.1 mm and a volume of 0.1  $\mu\text{L}$ , the total number of Hydrogel Microparticles was calculated using the following formula:  $[\text{Hydrogel Microparticles} / \text{mL}] = (\sum \text{Hydrogel Microparticles counted in } N \text{ squares}) \times \text{dilution factor} \times 10^4 / N$ ; where the  $10^4$  is the conversion from 0.1  $\mu\text{L}$  to 1 mL<sup>6</sup>.

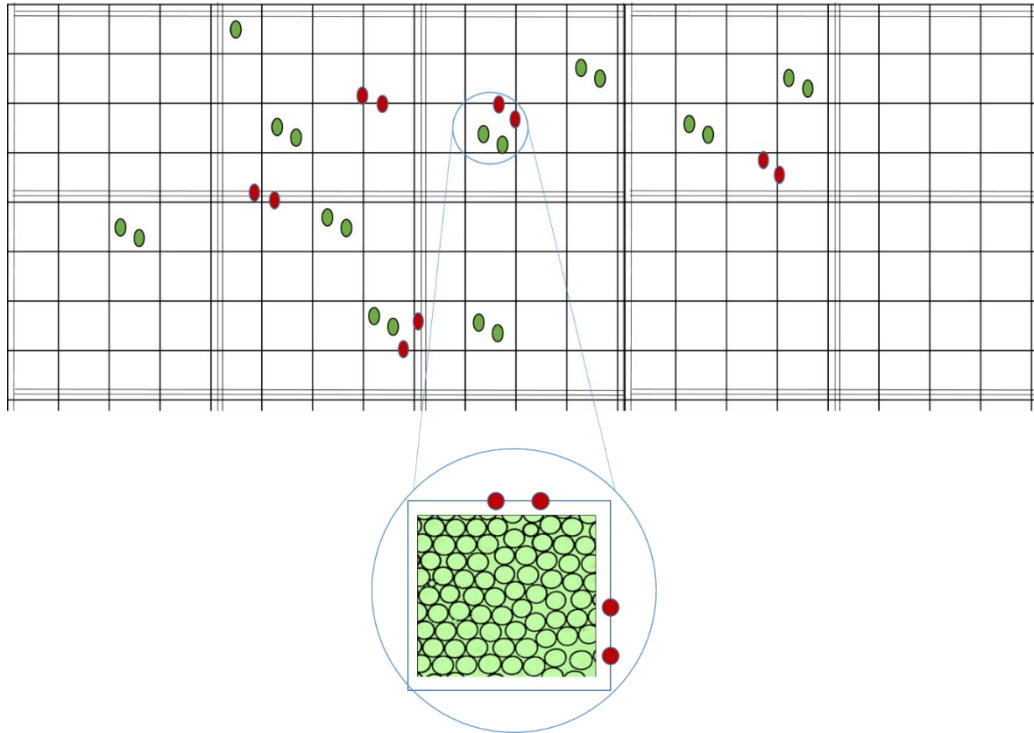
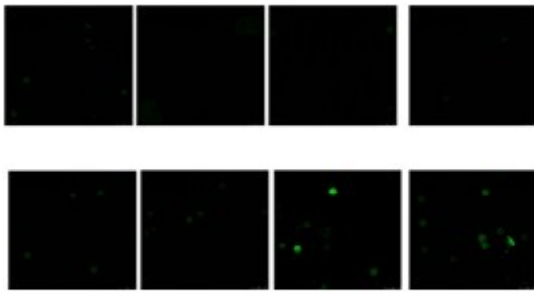


**Figure S13:** Schematic representation of Hydrogel Microparticles counting chamber. In order to avoid the risk of over- or under-counting Hydrogel Microparticles, only Hydrogel Microparticles on either side (green) have been counted.

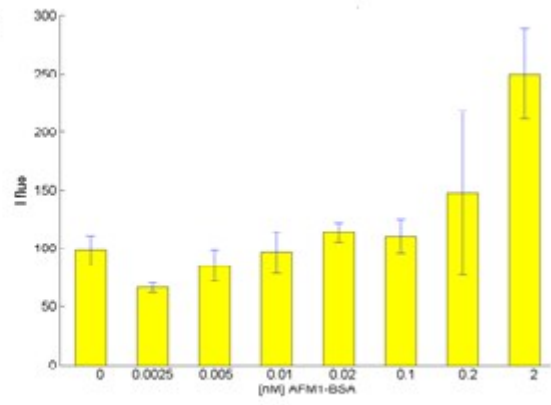
### 8. Confocal Microscopy and AFM1-BSA detection both in PBS and in Milk

Fluorescence analysis of AFM1 binding were performed by Leica SP5 confocal microscope (Leica Microsystems), provided with an HCX IRAPO L 25.0x/0.95 WATER objective and a 360 nm as selected wavelength as excitation sources for AFM<sub>1</sub>-BSA and the only AFM<sub>1</sub>. Detection occurred at the 420-450 nm band. Images have been acquired with a resolution of 1024 × 1024 pixels, zoom 1, 2.33 A.U. pinhole. All our experiments were performed at room temperature. Binding experiments were performed incubating different aliquots of peptide functionalized Hydrogel Microparticles with AFM<sub>1</sub>-BSA in PBS (pH 7.4) and milk (final volume 100 μL) at room temperature for 2 h. All samples were prepared adding different concentrations of AFM<sub>1</sub>-BSA, ranging from 0.0025 nM to 2 nM both in PBS and milk. After the incubation their fluorescence was analysed by confocal laser scanning microscopy (Figure S14A-B-C-D-E-F and Figure S15 A-B-C-D). No toxin capture were obtained for NDNR-Hydrogel Microparticles, but it showed a non-specific binding towards AFM<sub>1</sub>, both in PBS buffer and milk solution, (data not shown for milk solution). The same protocol was used for Hydrogel Microparticles without peptide functionalization, as a negative control (**Figure S14** G-H and **Figure S15** E-F).

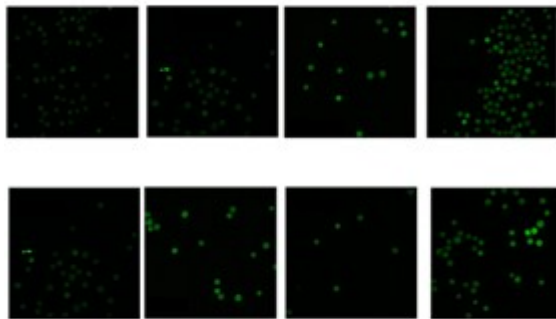
A



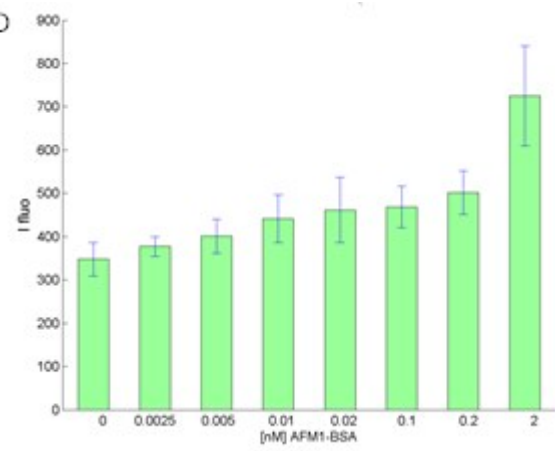
B



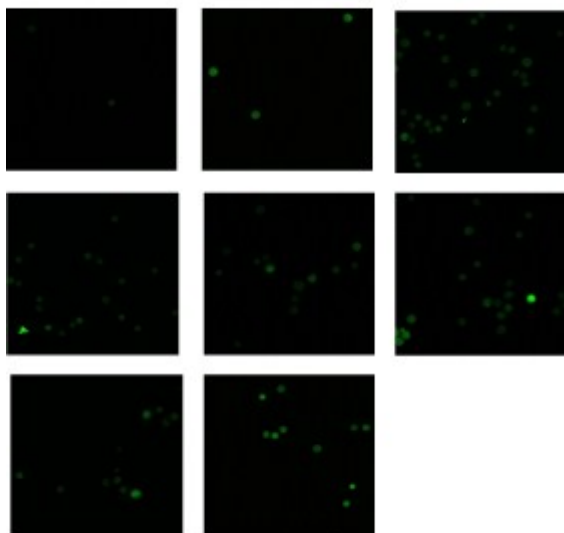
C



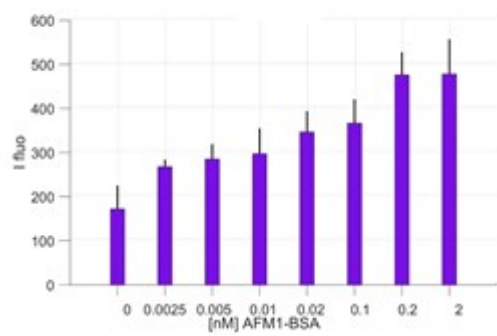
D

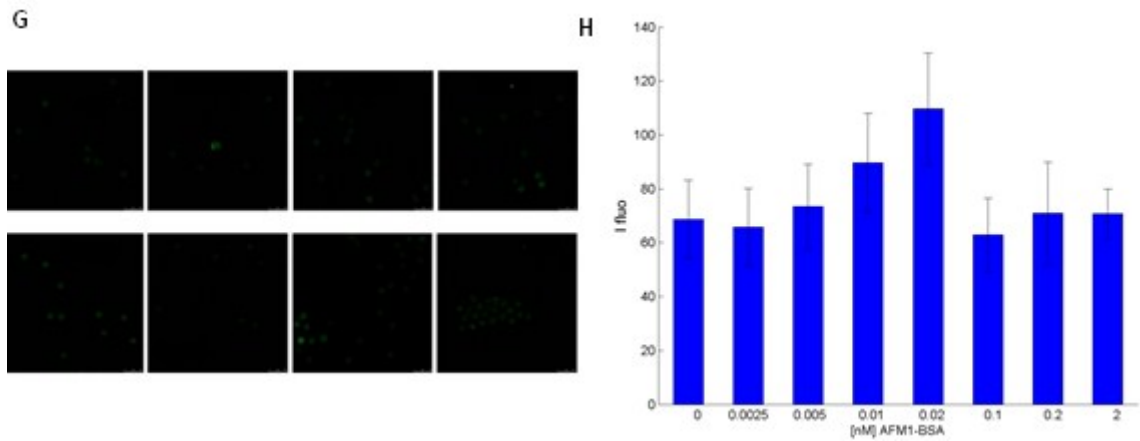


E

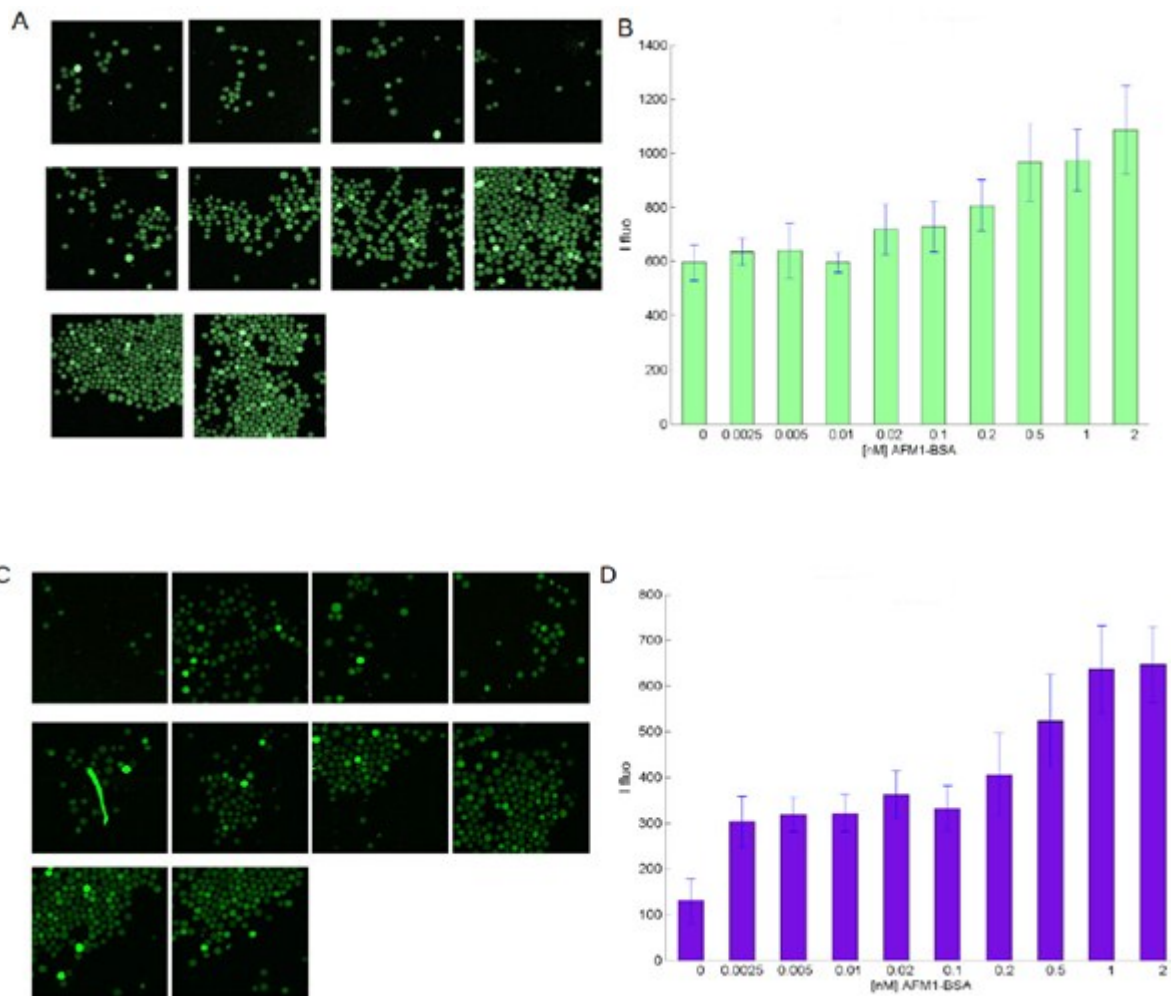


F





**Figure S14:** Multiphoton confocal images and quantification of singleHydrogel Microparticles fluorescent intensity using ImageJ tools, resulting from the binding between Aflatoxin M1-BSA conjugated (from 0.0025 nM to 2 nM) and A) NDNR-, C) NDDR-, E) NDPR-, G) control-Hydrogel Microparticles in PBS buffer; Excitation laser 700nm, emission 400-500nm. B-D-F) and H) Plot of fluorescent signal from AFM1-BSA excitation in NDNR-, NDDR-, NDPR- and control-Hydrogel Microparticles as function of AFM1-BSA concentrations in PBS buffer.



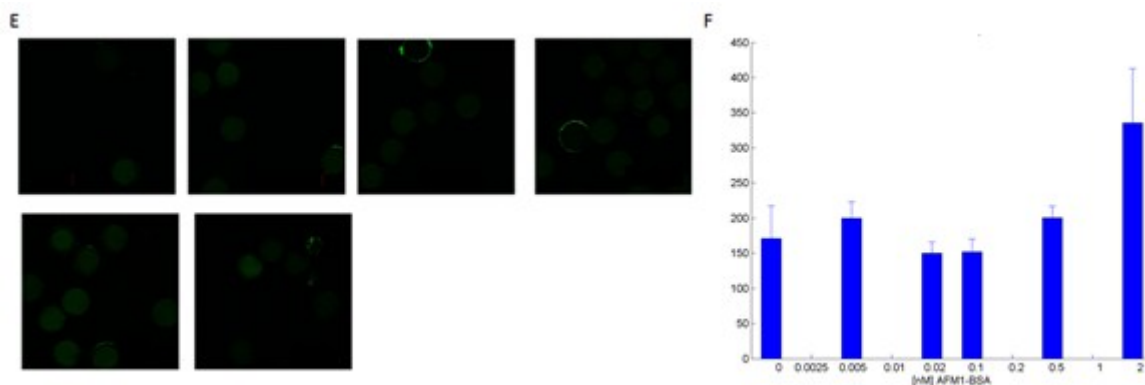


**Figure S15:** Multiphoton confocal images and quantification of single Hydrogel Microparticles fluorescent intensity using ImageJ tools, resulting from the binding between Aflatoxin M1-BSA conjugated (from 0.0025 to 2nM) and A) NDDR-, C) NDPR- and E) control-Hydrogel Microparticles in milk. Excitation laser 700nm, emission 400-500nm. B-D-F) Plot of fluorescent signal from AFM1-BSA excitation in NDDR-, NDPR-, control-Hydrogel Microparticles as function of AFM1-BSA concentrations in milk solution.

### 9. AFM<sub>1</sub>-BSA conjugated detection in Milk using different concentrations of Hydrogel Microparticles

In order to improve the sensibility of our biosensor, we decided to change Hydrogel Microparticles numbers in binding experiments. A dilution of 1:10 about Hydrogel Microparticles solution was used to perform new binding experiments, in this case the number of Hydrogel Microparticles in contact with aflatoxin was about 80 (the number of Hydrogel Microparticles was calculated as reported in S7 paragraph). Using a lower number of Hydrogel Microparticles, we were able to improve biosensor sensibility in aflatoxin recognition at very low concentrations (**Figure S16** A-B). On the basis of these new results, we can confirm that our system could be a promising tool for aflatoxin detection in milk samples.

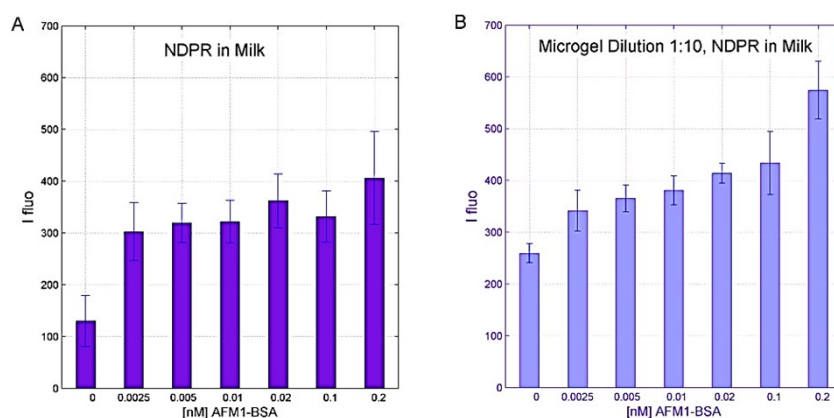


**Figure S16:** Binding between Aflatoxin M1-BSA conjugated and NDPR-Hydrogel Microparticle using a number of Hydrogel Microparticles diluted 1:10. A-B) Comparison of fluorescence signal between NDPR- and NDPR-Hydrogel Microparticles, diluted 1:10 after AFM1 binding. Using a lower number of Hydrogel Microparticles, there was an improvement on biosensor sensitivity.

## 10. AFM<sub>1</sub> detection directly in Milk.

With the aim to confirm the real specificity and sensibility of our biosensor, a binding assay between NDPR-, NDDR-Hydrogel Microparticles and the only Aflatoxin M1 (without BSA conjugation) was performed. For this experiment four different concentrations of aflatoxin were used: 0, 0.01, 0.1, 2nM. All images were performed by multiphoton confocal scanning microscopy using 700 nm as excitation laser, and 400-500 nm as emission band. The quantification of Aflatoxin M1 into Hydrogel Microparticles was performed by ImageJ tools, analyzing the fluorescence of the single microgel. As it is possible to see in **Figure S17B**, the assay developed in this work was able to recognize aflatoxin contamination in milk sample in a very specific manner only for the NDPR-Hydrogel Microparticles, unlike the NDDR-Hydrogel Microparticles that showed a very similar fluorescence signal for all concentrations (**Figure S17-A**).

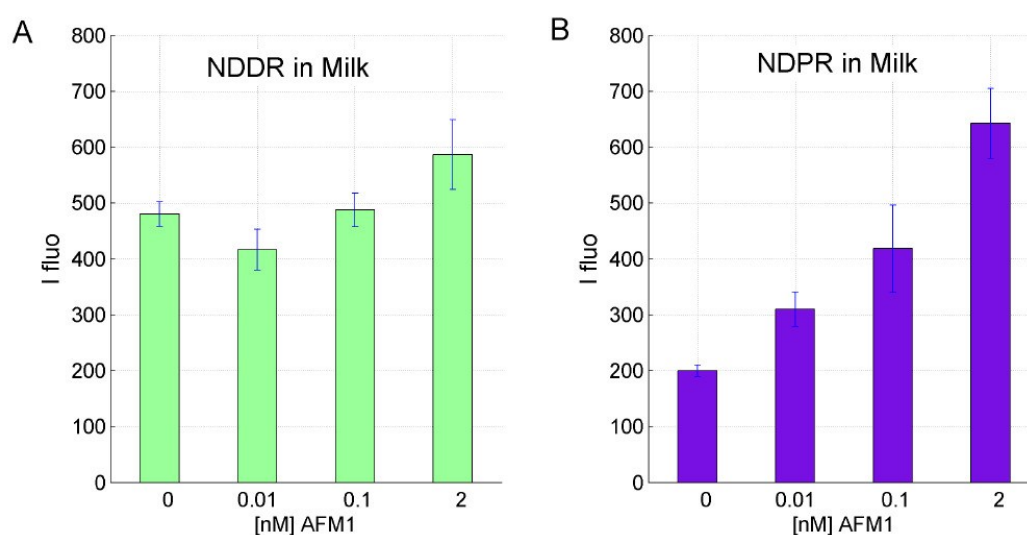


**Figure S17:** Binding assay between NDDR, NDPR-Hydrogel Microparticles and Aflatoxin M1 in milk sample. A) Plot of fluorescent signal of single Hydrogel Microparticles using ImageJ tools, resulting from the binding between Aflatoxin M1 (0nM, 0.01nM, 0.1nM and 2nM) and NDDR-Hydrogel Microparticles in milk sample. B) Plot of fluorescent signal from AFM1 excitation in NDPR-Hydrogel Microparticles in milk solution.

## 11. NDPR binding with different hydrophobic small molecules

In order to evaluate the NDPR peptide specificity towards AFM1, we used CDocker algorithm to calculate the Interaction Energy with two different hydrophobic small molecules such as cholesterol and coumarin. Coumarin was chosen as the basic molecular structure of all aflatoxins, while cholesterol is one of the most abundant components in milk. Only one illustrative picture of the 500 poses was reported in the **Figure S18 A-B-C**. The results demonstrate that both hydrophobic small molecules recognize the NDPR sequence with a low affinity, showing Interaction Energy values higher than that calculated for the interaction NDPR/AFM1 (Interaction Energy= -14.23 Kcal/mol for cholesterol/AFM1 and -11.37 Kcal/mol for coumarin/AFM1).

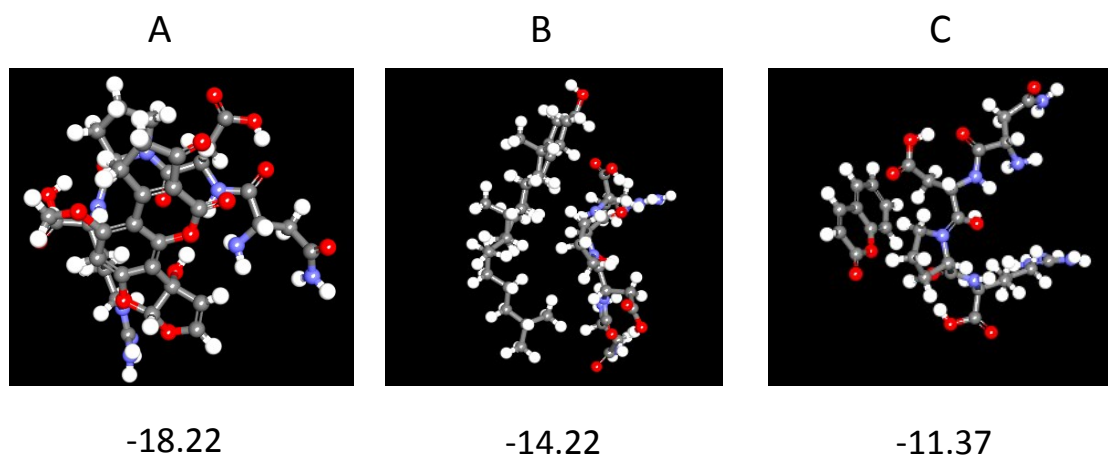


**Figure S18:** Interaction Energy values of A) NDPR/AFM1, B) NDPR/cholesterol and C) NDPR/coumarin complexes. Values are reported as Kcal/mol.

## 12. LoD values calculations

For the micro particle-based assay in the buffer (Fig. 4A and S14 F), the limits are calculated as follow:

$$\text{LoB} = 172 + 1.645(52) = 257.54$$

$\text{LoD} = 257.54 + 1.645(6.8) = 268.73$ , corresponding to a concentration of 2.38 pM according the equation of linear fitting of the lower concentrations

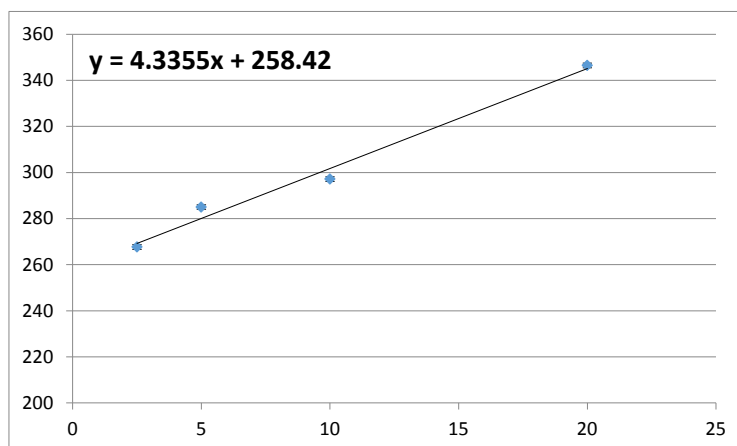


**Figure S19:** LoD calculations for NDPRD(O-allyl) hydrogel microparticles and the toxin dissolved in PBS buffer

Whereas for the micro particle-based assay in the milk (Fig. 4B and S15 D), the limits are calculated as follow:

$$\text{LoB} = 130 + 1.645(48.8) = 210.27$$

$\text{LoD} = 210.27 + 1.645(57.2) = 304.4$ , corresponding to a concentration of 2.46 pM according the equation of linear fitting of the lower concentrations

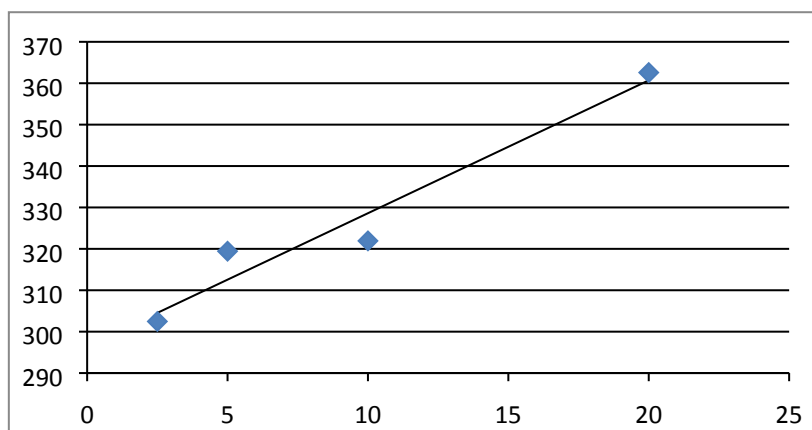


**Figure S20:** LoD calculations for NDPRD(O-allyl) hydrogel microparticles and the toxin dissolved in Milk solutions

These detection limits have been confirmed by analyzing the observed values for samples containing the LoD concentration. All these values are more than the LoB.

## REFERENCES

1. Wu, G.; Robertson, D. H.; Brooks, C. L.; Vieth, M., Detailed analysis of grid-based molecular docking: A case study of CDOCKER—A CHARMM-based MD docking algorithm. *Journal of computational chemistry* **2003**,*24* (13), 1549-1562.
2. (a) Rao, P. P.; Mohamed, T.; Osman, W., Investigating the binding interactions of galantamine with  $\beta$ -amyloid peptide. *Bioorganic & medicinal chemistry letters* **2013**,*23* (1), 239-243;(b) Rao, P. P.; Mohamed, T.; Teckwani, K.; Tin, G., Curcumin binding to beta amyloid: a computational study. *Chemical biology & drug design* **2015**,*86* (4), 813-820.
3. Reis, C. P.; Ribeiro, A. J.; Neufeld, R. J.; Veiga, F., Alginate microparticles as novel carrier for oral insulin delivery. *Biotechnology and bioengineering* **2007**,*96* (5), 977-989.
4. Tkachenko, A.; Xie, H.; Franzen, S.; Feldheim, D. L., Assembly and characterization of biomolecule-gold nanoparticle conjugates and their use in intracellular imaging. In *Nanobiotechnology protocols*, Springer: 2005; pp 85-99.
5. (a) Udenfriend, S.; Stein, S.; Boehlen, P.; Dairman, W.; Leimgruber, W.; Weigele, M., Fluorescamine: a reagent for assay of amino acids, peptides, proteins, and primary amines in the picomole range. *Science* **1972**,*178* (4063), 871-872;(b) Lorenzen, A.; Kennedy, S. W., A fluorescence-based protein assay for use with a microplate reader. *Analytical biochemistry* **1993**,*214* (1), 346-348;(c) De Bernardo, S.; Weigele, M.; Toome, V.; Manhart, K.; Leimgruber, W.; Böhlen, P.; Stein, S.; Udenfriend, S., Studies on the reaction of fluorescamine with primary amines. *Archives of biochemistry and biophysics* **1974**,*163* (1), 390-399.
6. Gunetti, M.; Castiglia, S.; Rustichelli, D.; Mareschi, K.; Sanavio, F.; Muraro, M.; Signorino, E.; Castello, L.; Ferrero, I.; Fagioli, F., Validation of analytical methods in GMP: the disposable Fast Read 102<sup>®</sup> device, an alternative practical approach for cell counting. *Journal of translational medicine* **2012**,*10* (1), 112.
7. D. A. Armbruster and T. Pry, Limit of Blank, Limit of Detection and Limit of Quantitation. *The Clinical Biochemist Reviews*, 2008, 29, S49.